Chronostratigraphy, composition, and origin of Ni-rich spinel from the Late Eocene Fuente Caldera section in Spain: One impact or more?

Eric ROBIN[1][*] and Eustoquio MOLINA[2]

[1]LSCE/IPSL, UMR CEA/CNRS 1572, Avenue de la Terrasse 91190 Gif-sur-Yvette, France
[2]Departamento de Ciencias de la Tierra, Universidad de Zaragoza, 50009 Zaragoza, Spain
[*]Corresponding author. E-mail: robin@lsce.cnrs-gif.fr

Abstract–Here we report on the stratigraphic distribution and chemical composition of Ni-rich spinel, a specific mineral tracer of meteorite impacts, in the Fuente Caldera section in Spain. A major peak in spinel abundance is observed in a biostratigraphic interval defined by the last occurrence of the planktic foraminifera *Porticulasphaera semiinvoluta* and the first occurrence of the planktic foraminifera *Turborotalia cunialensis*. Two other peaks of lower abundances are observed higher up in the same biostratigraphic interval, but geochemical considerations suggest that they likely originate from redeposition by turbiditic currents. Biostratigraphic correlations with the global stratotype section and point for the Eocene/Oligocene boundary of Massignano in Italy give an age of 35.4 ± 0.2 Ma (1σ) for the major peak. This age is indistinguishable from the age of the impact horizon at Massignano (35.5 ± 0.2 Ma) and within the age uncertainties for the Popigai (35.7 ± 0.2 Ma) and Chesapeake Bay (35.5 ± 0.5 Ma) craters. The Fuente Caldera spinel, as the Massignano spinel, is assumed to be a relic mineral of microkrystites, which are believed to derive from a unique source related to the Popigai impact crater. The morphologies and Cr compositions of the Fuente Caldera and Massignano spinel crystals are markedly different, however: the Fuente Caldera spinel occurs mostly as octahedral and skeletal crystals with 85% of the grains belonging to the Cr-rich magnetite series and 15% to the Fe-rich chromite series, whereas the Massignano spinel occurs mostly as dendritic crystals with 90% of the grains belonging to the Cr-poor magnetite series. It is unlikely that these differences are the result of post-depositional alteration processes because the compositions of the crystals, as well as their morphologies, are in general very similar to those reported for primary spinel crystals, i.e., spinel crystals present in meteorite fusion crust or synthetized from meteoritic material. In addition, spinel crystals have quite homogeneous compositions except for a few grains (<10%) showing Cr zonations, but these are assigned to primary crystallization processes. One possible explanation that is consistent with a single impact event producing spatial variations in spinel compositions and morphologies is that microkrystites are locally generated by the ablation in the atmosphere of impact debris. An alternative explanation is that Fuente Caldera and Massignano microkrystites derive from two closely spaced impact events, which however requires another, so-far unknown source crater for microkrystites.

INTRODUCTION

Impact horizons have been reported in a number of Upper Eocene sections but their number, geographic extent, and age, as well as their relationship with the two major Late Eocene impact craters, the Popigai in Siberia (>100 km in diameter) (Masaitis et al. 1999) and the Chesapeake Bay in northeastern America (40–90 km in diameter) (Koeberl et al. 1996; Collins and Wünnemann 2005), have been the subject of debate for many years. A review of the literature shows that at least two (Glass et al. 1985; Wei 1995), possibly three or four (Keller et al. 1987; Hazel 1989; Glass 1990; Molina et al. 1993; Montanari et al. 1993; Bodiselitsch et al. 2004), and up to six (Hazel 1989) impact horizons are supposed to have occurred in sediments from various sections of Late Eocene age. These horizons are characterized by the occurrence of microtektites and microkrystites (Glass et al. 1973, 1982, 1985, 1987, 2004b; John and Glass 1974; Keller et al. 1987; Glass and Koeberl 1999; Vonhof and Smit 1999) often associated with shocked quartz (Glass and Wu 1993; Clymer

et al. 1996; Langenhorst and Clymer 1996), Ni-rich spinel (Glass et al. 1985, 2004a; Pierrard et al. 1998, 1999; Pierrard 1999; Vonhof and Smit 1999), unusually high iridium concentrations (Asaro et al. 1982; Ganapathy 1982; Glass et al. 1985; Keller et al. 1987; Montanari et al. 1993; Pierrard et al. 1998; Pierrard 1999; Bodiselitsch et al. 2004), and a prominent anomaly of ^{3}He (Farley et al. 1998; Pierrard 1999).

Microtektites are glassy spherules devoid of crystalline inclusions, whereas microkrystites are spherules containing primary crystallites, i.e., crystal-bearing spherules. The Upper Eocene microkrystites contain clinopyroxene as the major crystalline phase with a minor amount of Ni- and Cr-rich spinel crystals (Glass et al. 1985, 2004b; Glass and Burns 1988). In the different horizons reported in the literature, no separation is found between microtektites and microkrystites (in a given horizon both components are usually mixed together in various proportions) except in Caribbean deep-sea core RC9-58 (John and Glass 1974), DSDP site 612 (Glass 1989; Glass et al. 1998), ODP sites 903 and 904 (Glass et al. 1998), and at Gay's Cove North on Barbados (Pierrard 1999) where microkrystites (or microkrystite remnants) are observed in a layer lying slightly below a microtektite layer, suggesting at least two impacts separated by a time interval of about 10–20 kyr (Glass et al. 1985). The microtektite horizon from these sites is believed to be part of the North American tektite strewn field (Glass et al. 1973; Glass 1989), the origin of which has been ascribed to the Chesapeake Bay impact in northeastern America (Koeberl et al. 1996; Deutsch and Koeberl 2006).

Regarding microkrystites, recent isotopic evidence has been presented in support of a single horizon, global in extent, with a provenance from the Popigai impact structure (Whitehead et al. 2000; Liu et al. 2001). The microkrystites display a wide range of chemical and isotopic compositions which, in the past, was tentatively proposed as evidence for possible multiple source craters (Keller et al. 1987; Vonhof and Smit 1999) and is now believed to reflect the compositional diversity of the Popigai target rocks (Kettrup et al. 2003). Although we agree that the wide variability in the microkrystite compositions can be accounted for assuming a single impact on an heterogeneous target (and if so, the Popigai seems to be the best candidate), it is, however, still unclear whether the different microkrystite layers reported so far in the literature all derive from a single, reworked, impact horizon or from a series of temporally closely spaced impact horizons. A detailed study of the stratigraphic distribution of impact spherules in Upper Eocene sections with high sediment accumulation rates would help to resolve this problem. However, the difficulty in extracting spherules without damage from compacted/altered sediments—which are more friable after diagenetic alteration (Glass et al. 2004a)—and in unambiguously identifying crystalline structures and interpreting compositional differences, can lead to counting loss, misidentification, and controversial conclusions (Glass and Burns 1987).

This has pushed us to study the stratigraphic distribution of Ni-rich spinel originally present in microkrystites (Glass et al. 1985, 2004a, 2004b). Indeed, spinel crystals can be extracted without damage from diagenetically altered sediments and then easily sorted and counted according to specific chemical criteria using an automated particle counting and classification system (Robin et al. 1991). Nickel-rich spinel differs from terrestrial spinel in its high nickel content, reflecting the high abundance of this element in the parent material, and a high ferric/ferrous ratio resulting from crystallization in an O_2-rich environment (Robin et al. 1992; Gayraud et al. 1996; Toppani and Libourel 2003). Spinel is found in meteorite fusion crusts, cosmic spherules from deep-sea sediments, and polar ice (Robin et al. 1992), and in a variety of impact debris in the sedimentary record: at the Cretaceous/Paleogene boundary (65 Myr ago) (Smit and Kyte 1984), in a Lower-Middle Jurassic hardground (~180 Myr ago) from the southern Alps in Italy (Jéhanno et al. 1988), in Late Pliocene sediments (~2 Myr ago) from the Antarctic basin (Margolis et al. 1991), in Oligocene sediments (~30 Myr ago) from the central North Pacific (Kyte and Bostwick 1995), and in the Global Stratotype Section and Point for the Eocene/Oligocene boundary of Massignano in Italy (Pierrard et al. 1998). Its occurrence in the sedimentary record thus provides strong evidence for an exceptional accretion event and may help in constraining the nature of this event (Robin et al. 1991).

In this paper, we present the stratigraphic distribution and chemical composition of Ni-rich spinel in the late Eocene Fuente Caldera section in Spain and discuss the implications regarding the number and age of late Eocene impact horizons as well as their potential source craters.

SITE DESCRIPTION, STRATIGRAPHY, AND SAMPLING

The Fuente Caldera section is located in the Gavilan ravine, one kilometer northeast of the Fuente Caldera farmhouse, in the township of Pedro Martinez in the northern part of the Granada province (southern Spain) (Fig. 1). This is a sequence of hemipelagic marls interbedded with several sandstone layers of turbiditic origin. The studied sequence is 109 m thick, spanning about 3 Myr from the upper Eocene to the basal Oligocene, and is apparently complete according to biostratigraphic studies (Molina 1986; Monechi 1986; Molina et al. 2004). A relatively precise chronostratigraphy for this sequence was established using biostratigraphic correlations between the Fuente Caldera section and the Global Stratotype Section and Point (GSSP) for the Eocene/Oligocene boundary of Massignano in Italy (Fig. 2). Sediment accumulation rates calculated over different biostratigraphic intervals are relatively constant with an average value of 39.3 ± 3.6 m Myr^{-1} suggesting a continuous sedimentation history with no major hiatus (>200 kyr) for this sequence. However, the occurrence of numerous sandstone layers of turbiditic origin
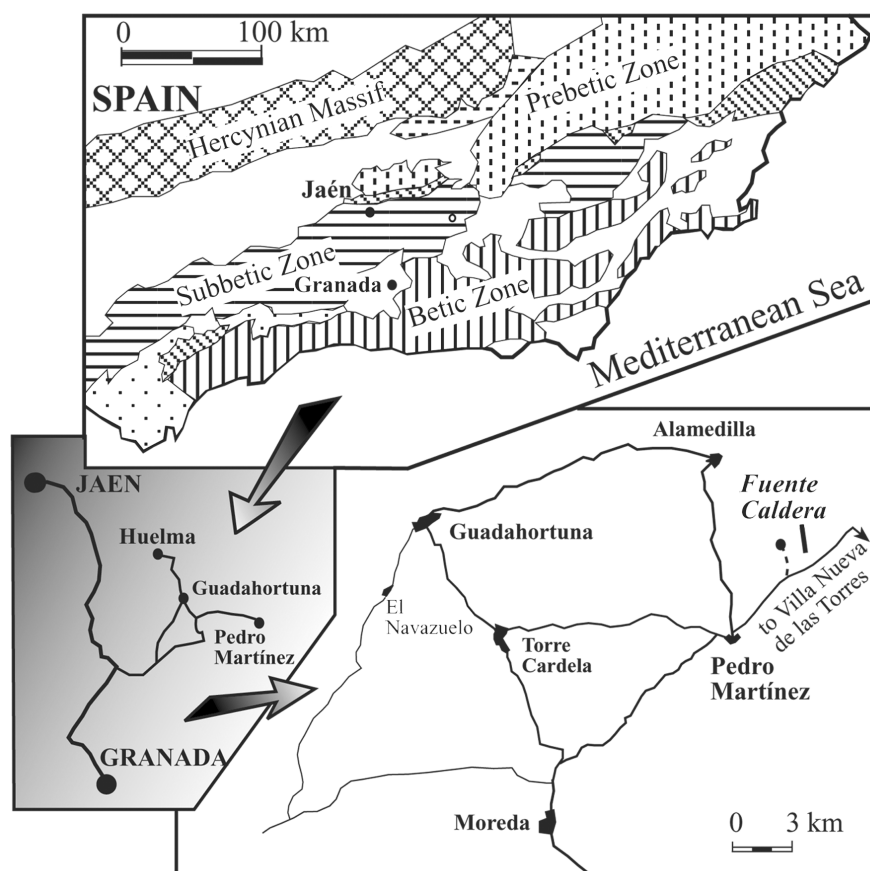
Fig. 1. A map showing the location of the Fuente Caldera section.

all along the sequence is indicative of possible erosion, transport, and redeposition and we cannot exclude some minor hiatus (<200 kyr). Assuming no hiatus, the temporal resolution for this section is defined by the time required for the deposition of a sediment thickness equal to the sampling interval and is limited to the time required for the deposition of a sediment thickness equal to the bioturbation depth (about 10 cm). Two events separated in time by less than the temporal resolution cannot be distinguished in the sedimentary record.

A continuous sampling was performed by integrating rock material over stratigraphic intervals of 25–70 cm corresponding to temporal resolutions of 6–18 kyr (Table 1). Note that the best available temporal resolution at Fuente Caldera is 2.5 kyr, assuming a maximum bioturbation depth of 10 cm. At Massignano, the sedimentation rate is about 5 times lower (8.3 ± 0.5 m/Myr) leading to a maximum temporal resolution of about 12 kyr. Sampling was performed from the last occurrence of the planktic foraminifera *Porticulasphaera semiinvoluta* to the first occurrence of the planktic foraminifera *Turborotalia cunialensis*. This interval corresponds to the 3 m biostratigraphic interval in the GSSP of Massignano where a huge Ni-rich spinel peak has been reported (Pierrard et al. 1998).

ANALYTICAL METHODS

The concentration of Ni-rich spinel crystals in Eocene samples was determined following the procedure described by Robin et al. (1991). The samples (about 1 kg of rock material) were crushed and homogenized in an agate mortar. About 3–4 g of powdered sample were then ultrasonically disaggregated in 10% acetic acid and the magnetic particles were collected with a magnet and recovered on a 0.5 µm nuclepore filter. Nickel-rich spinel crystals larger than 0.5 µm were sorted and counted using an automatic search routine called the Automated Chemical Classification (ACC) system on a JEOL 840 scanning electron microscope (SEM) associated with an energy dispersive spectrometer (EDS) from Princeton Gamma Tech (PGT). Spinel recovery and counting efficiencies were tested by adding to the starting material a known amount of Mn-rich synthetic spinel crystals and range from 50 up to 95%.

The ACC system works as follows: a numerical image is first obtained from the backscattered electron beam. Typical image resolution and magnification are 1024×1024 pixels and 1000×, respectively, well-suited for the detection of particles ranging from 0.5 µm up to 20 µm. The image is then binarized, filtered, and a threshold is applied to remove from
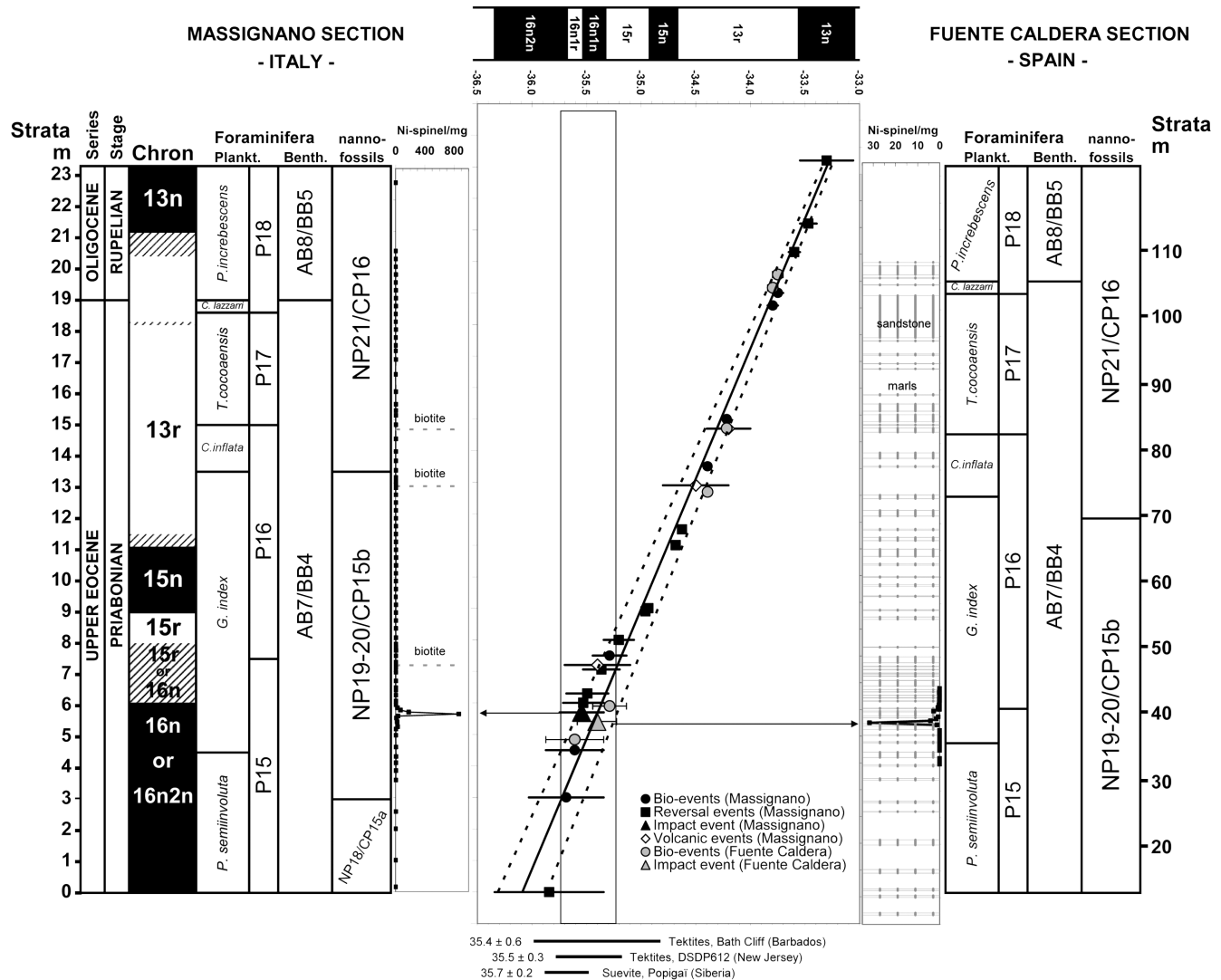
Fig. 2. The chronology of the Fuente Caldera section, established from the biostratigraphy of this sequence (Molina 1986; Molina et al. 2004; Monechi 1986) and the magnetostratigraphy (Bice and Montanari 1988; Lowrie and Lanci 1994) and biostratigraphy (Coccioni et al. 1988) for the GSSP of the Eocene/Oligocene boundary at Massignano, assuming the same age for the biostratigraphic events in both sequences. Also shown are the radiometric ages and related uncertainties of 1) three volcanic ash layers from the Massignano section in Italy (Montanari et al. 1993), 2) tektite fragments from DSDP site 612 in the North Atlantic off New Jersey (Obradovich et al. 1989) and the Bath Cliff section in Barbados (Glass et al. 1986), and 3) suevite samples from the Popigai in Siberia (Bottomley et al. 1997). The regression line (plain line) gives the correspondence between stratigraphic levels (m) and absolute ages (Myr) for both Massignano and Fuente Caldera sections, and the dashed lines give the corresponding uncertainties. In the two columns showing the stratigraphic distributions of spinel crystals, the vertical patterns indicate sandstone layers and no pattern indicates marl.

the image all particles that are not magnetite (mainly calcareous, siliceous, and clay-rich minerals, which have been recovered together with the magnetic particles). The threshold is adjusted from a reference image showing different minerals (magnetite, carbonate, and silicate) in such a way that the less dense minerals (carbonate and silicate) are removed from the image displaying magnetite only.

In the first step, the position and shape parameters (perimeter P, area A, longest and shortest dimensions, L and l, respectively, and the average diameter d_{avg} = mean of 12 directed diameter) of the particles remaining on the

backscattered image are determined and stored. The particle size is then defined as the area-equivalent diameter, which is the diameter expressed as a function of the area of the particle ($AED = [4A/\pi]^{1/2}$ with A being the measured particle area). The AED gives an average value of the particle diameter, well-suited for the determination of the particle size and mass distributions, but it is important to note that AED is not representative of the maximum dimension of the particle. This latter can be expressed as a function of the particle size through the elongation ratio that is defined as the ratio of the longest (L) and shortest (l) dimensions of each individual

Table 1. Age, concentration, and total flux of Ni-rich spinel at Fuente Caldera.

Sample	Strata (Z in m)	Calculated age (Myr)	Sampling interval (ΔZ in cm)	Temporal resolution (Δt in kyr)	Concentration C^a (crystals/mg)	Flux Φ^b ($\times 10^4$ crystals/ cm^2)
Sandstone 9.1.0.						
FC-A	32.02	−35.578	25	6	<0.05	
FC-B	32.29	−35.571	25	6	<0.05	
FC-C	32.56	−35.564	30	8	<0.05	
FC-D	32.85	−35.557	30	8	<0.05	
Sandstone 9.1.1.						
FC-E	34.05	−35.526	50	13	<0.05	
FC-F	34.45	−35.516	30	8	<0.05	
FC-G	34.73	−35.508	30	8	<0.05	
FC-H	35.02	−35.501	30	8	<0.05	
Sandstone 9.1.2.						
FC-I	35.51	−35.488	33	8	<0.05	
FC-J	35.82	−35.480	33	8	<0.05	
FC-K	36.13	−35.472	34	9	<0.05	
Sandstone 9.1.3.						
FC-L	36.53	−35.462	33	8	<0.05	
FC-M	36.79	−35.455	33	8	<0.05	
FC-N	37.05	−35.449	34	9	<0.05	
Sandstone 9.1.4.						
FC-O	37.87	−35.427	70	18	1.21 ± 0.21	6.07 ± 1.05
FC-P	38.19	−35.419	30	8	31.68 ± 2.51	144.36 ± 11.42
FC-Q	38.50	−35.411	30	8	4.14 ± 0.50	18.85 ± 2.28
FC-R	38.80	−35.404	30	8	1.61 ± 0.28	7.09 ± 1.23
Sandstone 9.1.4b.						
FC-S	39.09	−35.396	30	8	0.71 ± 0.13	2.79 ± 0.49
Sandstone 9.1.5.						
FC-T	39.93	−35.375	30	8	2.74 ± 0.34	10.76 ± 1.33
FC-U	40.19	−35.368	30	8	0.16 ± 0.06	0.62 ± 0.24
Sandstone 9.1.5b.						
FC-V	40.48	−35.360	70	18	0.77 ± 0.16	2.41 ± 0.49
FC-W	40.69	−35.355	70	18	0.11 ± 0.05	0.33 ± 0.17
FC-X	40.90	−35.350	30	8	0.26 ± 0.09	0.81 ± 0.29
FC-Y	41.11	−35.344	30	8	0.14 ± 0.06	0.45 ± 0.20
FC-Z	41.32	−35.339	30	8	0.14 ± 0.08	0.43 ± 0.25
Sandstone 9.1.6.						
FC-AA	41.53	−35.334	25	6	0.06 ± 0.04	0.09 ± 0.06
FC-AB	41.63	−35.331	25	6	0.16 ± 0.07	0.25 ± 0.10
FC-AD	41.84	−35.325	25	6	0.16 ± 0.06	0.25 ± 0.10
Sandstone 9.1.7.						
FC-AG	42.21	−35.316	30	8	0.03 ± 0.03	0.05 ± 0.05
Sandstone 9.1.8.						
FC-AH	42.42	−35.311	30	8	0.05 ± 0.04	0.17 ± 0.12
FC-AI	42.62	−35.306	30	8	0.14 ± 0.06	0.27 ± 0.12
FC-AJ	42.75	−35.302	30	8	0.20 ± 0.08	0.39 ± 0.16
Sandstone 9.1.8b.						
FC-AL	43.07	−35.294	30	8	0.05 ± 0.05	0.12 ± 0.12
Sandstone 9.1.8c.						
FC-AM	43.32	−35.287	40	10	<0.05	
Total in the peak (sample P)						144 ± 11
Total (samples O to AL)						197 ± 12

[a] Average concentration over the sampling interval; all errors at 2σ confidence limit.

[b] $\Phi = 10.C.\Delta Z.\rho$ with the density of the sediment $\rho = 1.5$ g/cm^3.

particle (see the Results section). For a circular particle, the elongation ratio is unity and the *AED* is the maximum dimension of the particle. For an irregularly shaped particle, the elongation ratio is larger than unity and the *AED* is smaller than the maximum dimension.

Note that particle size measurement accuracy and reproducibility are sensitive to i) particle recovery efficiency in the different size fractions and to ii) intensity variations of the electron beam, and are all the more sensitive as the particles are small. Since a majority of spinel grains are in the small size range (*AED* = 0.5–2 μm; see the Results section), it is important to warrant spinel recovery efficiency in the different size fractions as well as electron beam stability during the whole sample analysis. This is achieved by comparing the size distribution of the Mn-rich synthetic spinel crystals measured in the investigated sample to the one previously determined from replicate analyses of a pure reference sample. Particle size measurements are considered to be correct when the size distribution of the Mn-rich synthetic spinel crystals in the investigated sample falls within 2 sigma error bars of the reference values.

In the second step, an X-ray spectrum is acquired for each particle with an *AED* larger than 0.5 μm (minimum particle size required for X-ray spectrum acquisition at 15 kV) using a high purity germanium (HPGe) detector and digital pulse processing from PGT. Compared to traditional Si(Li) detectors equipped with analog electronics, HPGe and digital pulse processing provide superior resolutions at high count rates and low dead times, allowing low X-ray spectra acquisition times (typically less than 5 seconds) and thus quick identification of Ni-rich spinel from Ni, Fe, Mg, and O K lines. Terrestrial spinel crystals (magnetite, titanomagnetite, chromite, and titanochromite) are also sorted from the Fe, Ti, Cr, and O K lines. It is therefore possible to count and sort by size and composition several hundreds of spinel crystals of different origins in a few hours. Counting was generally made on 100 or more spinel crystals to minimize statistical uncertainty, and a minimum of two replicate samples were analyzed to test possible sample heterogeneity. The detection limit for Ni-rich spinel crystals >0.5 μm in diameter depends on the abundance of other magnetic grains, and thus may slightly vary from sample to sample. In Fuente Caldera samples, it is generally lower than 0.05 spinel crystal mg^{-1} (all concentrations are given per mass unit of whole rock sample).

In the third and last step, multi-element spectra obtained from the SEM/EDS-ACC system were compared to a series of pure reference spectra, and X-ray absorption and fluorescence effects were corrected using ZAF program supplied by PGT. This enabled us to carry out quantitative analyses for the elements Mg, Al, Ti, Cr, Mn, Fe, and Ni simultaneously. The precision is about 5% of the measured value and the sensitivity is 0.1 wt%.

Quantitative analyses are thus performed on grain

mounts that are not polished sections and this may result in two types of analytical artifacts: 1) X-ray absorption and fluorescence effects on irregularly shaped grains are difficult to constrain, which may affect ZAF corrections and, hence, the estimation of the spinel elemental abundances, and 2) the outermost part of the spinel grain only is analyzed, which may not reflect the composition of the whole grain. Note that these analytical artifacts become significant only for spinel crystals larger than 1 μm (maximum penetration depth of the electron beam in spinel at 15 kV), these latter representing up to 50% of the total population of spinel (see the Results section). To address this problem, two types of SEM/EDS-ACC analyses have been performed: grain exterior was first analyzed on a set of spinel crystals from Fuente Caldera and Massignano as well. The crystals were recovered as described above on two separate filters. The filters were then embedded in epoxy resin and grain interior was analyzed on polished sections obtained using diamond spray. These two types of analyses were also performed to tentatively address the problem of the possible alteration of the spinel crystals by comparing the composition of the exterior of the grains with that of the interior.

RESULTS

Vertical Distribution and Age

Results showing the stratigraphic distribution of Ni-rich spinel at Fuente Caldera are given in Table 1 and plotted in Figs. 2 and 3. Spinel was not detected (<0.05 crystal mg^{-1}) below the level of 38.20 m, where a major peak of 31.7 ± 2.5 spinel crystals mg^{-1} is observed in marly sediments, about 70 cm above sandstone layer 9.1.4. Biostratigraphic correlations with the GSSP of Massignano give an age of 35.4 ± 0.2 Myr for this horizon. Two other spinel peaks of 2.7 ± 0.3 and 0.8 ± 0.2 crystals mg^{-1} are observed higher up in the section at the top of sandstone layers 9.1.5 and 9.1.5b at 39.95 m and 40.5 m, respectively. These horizons are 44 ± 4 and 58 ± 5 kyr younger than the first one, assuming a constant sediment accumulation rate of 39.3 ± 3.6 m Myr^{-1}. Low but significant spinel overabundances (0.05–0.25 crystals mg^{-1}) are measured up to 43 m (≈35.3 Myr), then spinel remains undetectable in the rest of the investigated section (up to 44 m).

Spinel Size and Mass Distributions, Crystal Morphologies, and Total Flux

Figures 4a and 4b give the normalized cumulative size distribution and the differential mass distribution of Ni-rich spinel crystals at Fuente Caldera and Massignano. The normalized cumulative size distribution is defined as the number of spinel crystals larger than a given size normalized to the total number of spinel crystals, i.e., the number of spinel crystals larger than 0.5 μm. The differential mass
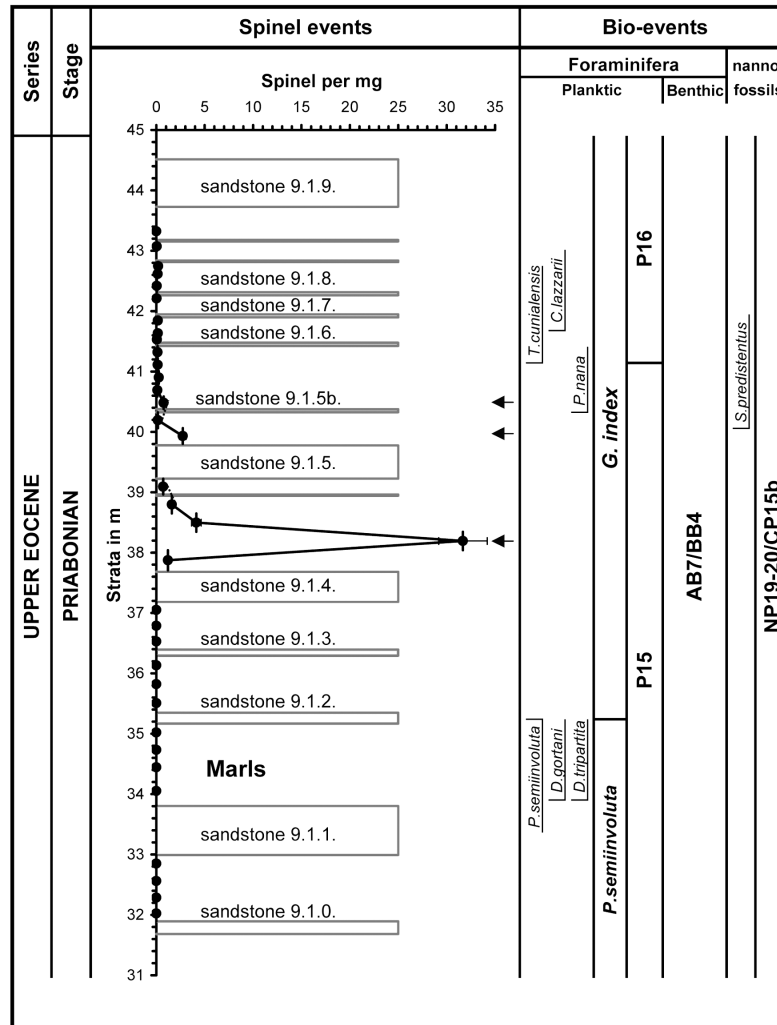
Fig. 3. A detailed stratigraphic distribution of spinel crystals at Fuente Caldera, Spain.

distribution is calculated from the cumulative size distribution and is normalized to the total mass of spinel according to the following equation:

$$M_{\text{spinel}}(x_1;x_2) = \left(\int_{x_1}^{x_2} V(x)\,dN_{\text{cumul}}(x) \right) \Big/ \left(\int_{0.5}^{+\infty} V(x)\,dN_{\text{cumul}}(x) \right) \quad (1)$$

where $N_{\text{cumul}}(x)$ is an exponential function that fits the cumulative size distribution and $V(x)$ is the volume of the particle. This one is assumed to be equivalent to the volume of a sphere having a diameter defined by the AED. It is about equivalent to the volume of a prolate spheroid, i.e., the volume of an elliptical grain rotated about its longest dimension.

The results show that no difference in the size and mass distribution is observed between Fuente Caldera and Massignano. Both size distributions are similar with typical grain sizes ranging from 0.5 (100%) up to 5 μm (<0.1%) and a majority of grains (up to ≈90%) in the 0.5–2 μm size range.

Both differential mass distributions are characterized by a rapid rise with a maximum around AED = 1.5–2.0 μm, followed by an exponentially decreasing tail. The distributions are relatively narrow with a full width at half maximum of about 2.5 μm corresponding to about 80% of the total spinel mass in the 1.0–3.5 μm size range. The total contribution of particles smaller than 1 μm and larger than 4 μm to the total spinel mass is less than 10 wt%.

A significant difference in the cumulative distribution of the L/l elongation ratio of spinel grains is observed between Fuente Caldera and Massignano, with a higher abundance of elongated crystals at Massignano (Fig. 4c). This difference is indicative of different crystal morphologies. This is confirmed by SEM observations showing that the Fuente Caldera spinel occurs mostly as compact grains with skeletal and well-developed octahedral morphologies (Figs. 5a–c), whereas the Massignano spinel occurs mostly as elongated grains with dendritic morphologies (Pierrard et al. 1998). The dendritic spinel morphology is also observed at Fuente
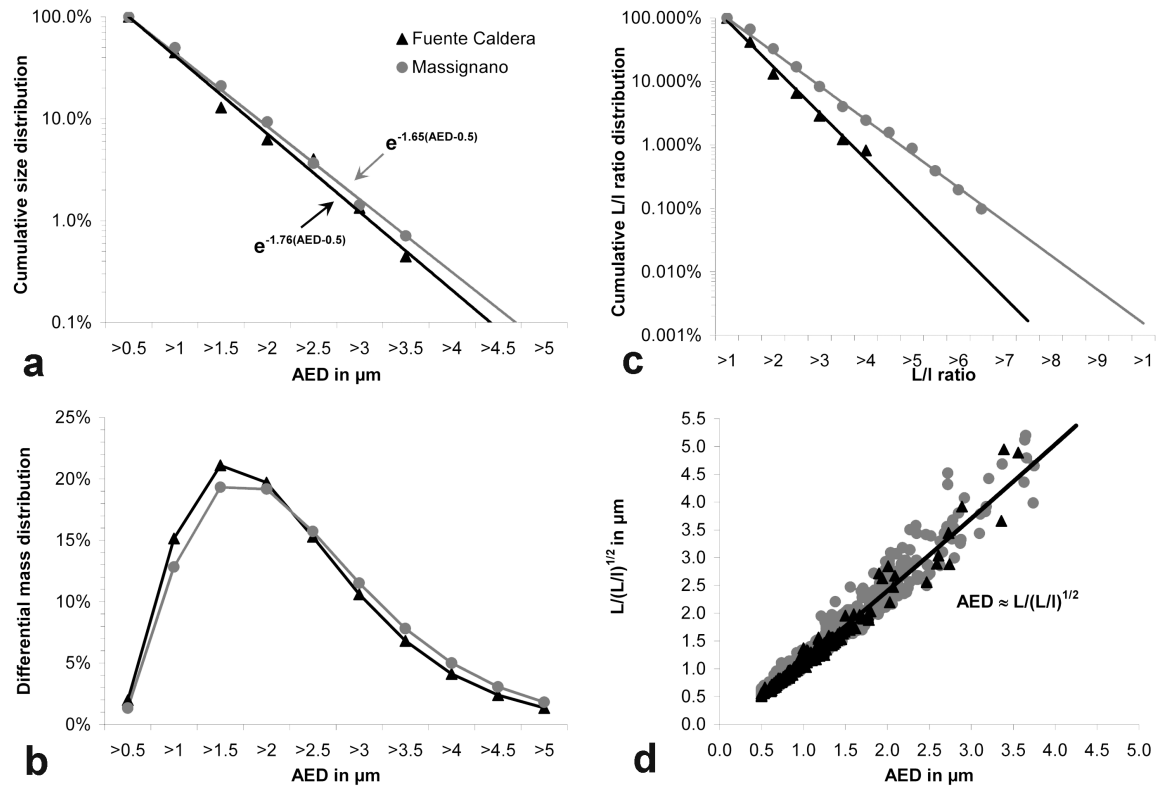
Fig. 4. a) Normalized cumulative size distributions of spinel crystals fitted with exponential functions; b) differential mass distributions calculated from the size distributions, volume, and density of the spinel crystals (see text); c) the normalized cumulative elongation ratio of spinel crystals calculated from the maximum (L) and minimum (l) dimensions of individual grains; and d) the relationship between the maximum dimension (L), the L/l elongation ratio, and the *AED*.

Caldera (Fig. 5d), though it is poorly represented at this site. For instance, the abundance of spinel grains with an elongation ratio larger than 5, which is typical of large dendritic crystals, is about 10 times lower at Fuente Caldera than at Massignano. At Massignano, Pierrard et al. (1998) reported the finding of very thin ($l \approx$ 1–2 µm) dendritic crystals with overall dimensions up to $L \approx$ 20 µm (L/l elongation ratio >10). Figure 4c shows that such large spinel crystals are rare, even at Massignano (less than 0.001%). Figure 4d shows the relationship between the maximum dimension (L), the L/l elongation ratio, and the *AED*. Note that a spinel grain with an L/l elongation ratio >10, and a maximum dimension $L \approx$ 20 µm, has an *AED* > 5 µm ($AED \approx L/(L/l)^{1/2} > 20/(10)^{1/2}$; Fig. 4d). The contribution of such large spinel grains to the total spinel mass is negligible (<3 wt%, Fig. 4b).

Considering the overall stratigraphic extent of the spinel distribution (≈4.6 m) at Fuente Caldera, the total integrated flux is about ≈2 × 10^6 crystals cm^{-2}, with the major peak contributing to ≈75% of this value (Table 1). Such a flux is comparable or higher to the fluxes measured at the Cretaceous/Paleogene boundary (≈3 × 10^3 to 5 × 10^6 crystals cm^{-2}) (Robin et al. 1991; Rocchia et al. 1996; Robin and Rocchia 1998). It is, however, 10 times lower than that one determined in the GSSP of Massignano (≈2 × 10^7

crystals cm^{-2}) (Pierrard et al. 1998). Note that the difference in the spinel flux between Fuente Caldera and Massignano is the same for the total mass than for the total number of crystals since both sites show similar particle size and mass distributions.

Spinel Compositions and Compositional Variations with Crystal Sizes and Morphologies

The average composition and compositional range of the spinel grains having an *AED* > 0.5 µm are given in Table 2 and the normalized differential distributions of their Cr contents are shown in Fig. 6. This figure shows that the Cr concentrations of the Fuente Caldera spinel in the different layers as well as in the background in the interval 38–43 m are all very similar but are markedly different from those of the Massignano spinel. The Fuente Caldera spinel is a Cr-rich spinel with 85% of the grains belonging to the Cr-rich magnetite series (*AED* > 0.5 µm; Cr_2O_3 between 15 and 35 wt%) (Fig. 7) and 15% to the Fe-rich chromite series (*AED* > 0.5 µm; Cr_2O_3 > 35 wt%). At the opposite, the Massignano spinel is a Cr-poor spinel that mostly belongs to the Cr-poor magnetite series (>90% of the grains with *AED* > 0.5 µm and Cr_2O_3 < 15 wt%, 70% of which with Cr_2O_3 < 5 wt%) with ≈5% of the grains only belonging to the Cr-rich magnetite
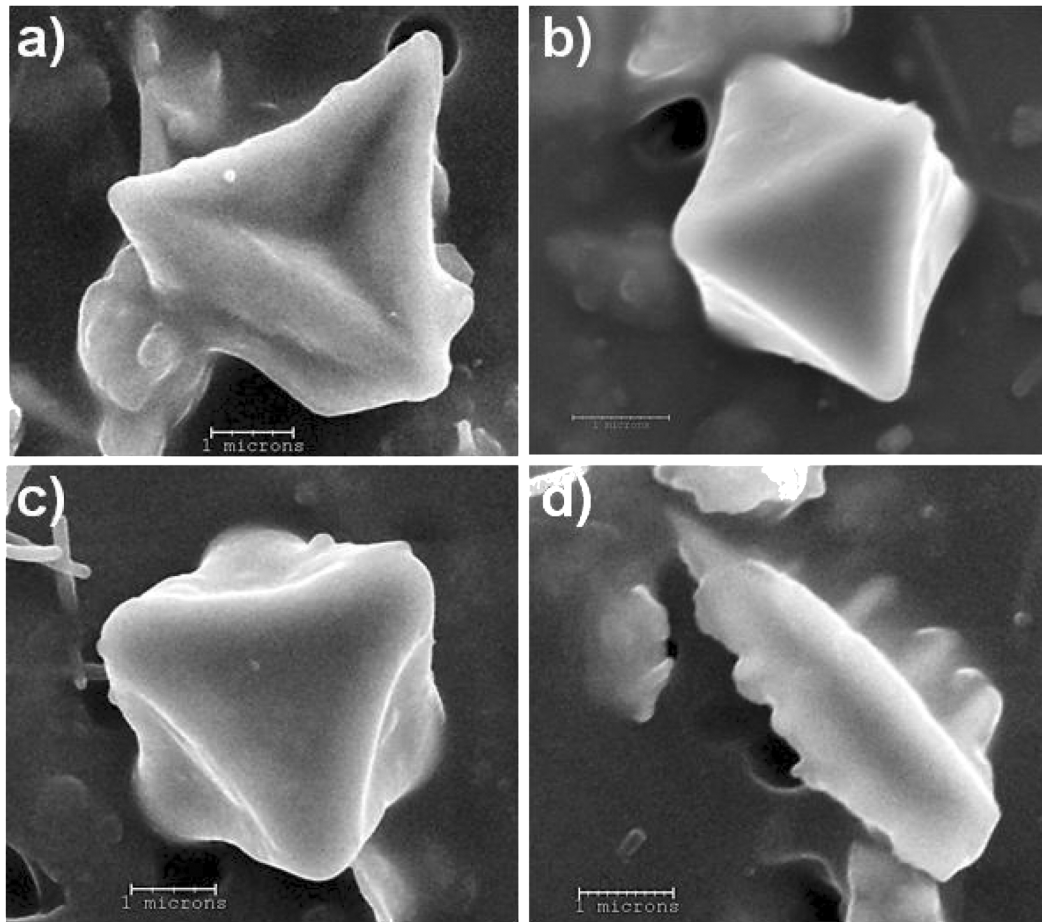
Fig. 5. SEM images of spinel crystals from Fuente Caldera, Spain. a–c) Skeletal and octahedral morphologies, the most common crystal habits, are indicative of crystallization from melt heated below liquidus (Gayraud et al. 1996). d) A rare dendritic crystal that is typical of rapid growing in nonequilibrium conditions.

Table 2. Chemical compositions of Ni-rich spinel at Fuente Caldera (Spain) and Massignano (Italy).

	Fuente Caldera						Massignano			
	38.2 m		39.95 and 40.5 m		Background 38–42.8 m		5.6–5.8 m			
	Grain interior		Grain exterior		Grain exterior		Grain exterior		Grain interior		Grain exterior	
	1866[a]		503[a]		273[a]		112[a]		1232[a]		1022[a]	
wt%	Mean	Range	Mean	Range	Mean	Range	Mean	Range	Mean	Range	Mean	Range
MgO	10.1	2.3–18.9	10.5	3.4–17.5	9.5	0.4–17.1	7.4	0.5–16.0	7.5	1.1–19.4	7.4	0.3–18.2
Al_2O_3	2.9	0.1–15.0	2.8	0.8–6.4	4.8	0.1–13.9	4.6	1.6–9.5	2.6	0.2–12.5	2.7	0.2–9.9
TiO_2	0.6	0.1–7.5	0.2	0.1–1.5	0.3	0.1–3.0	0.3	0.1–1.0	0.9	0.2–4.7	0.5	0.1–5.5
Cr_2O_3	25.7	13.2–53.5	25.0	14.7–51.2	23.6	5.5–51.0	21.9	4.4–39.7	4.9	0.1–42.8	4.6	0.1–29.3
MnO	0.3	0.1–1.8	0.4	0.1–0.9	0.4	0.1–7.8	0.5	0.1–1.6	0.3	0.1–1.9	0.3	0.1–1.0
FeO	13.8	0.2–27.0	13.4	1.4–22.7	15.5	4.3–30.4	17.2	0.9–28.4	17.7	0.1–28.2	17.9	2.2–30.2
Fe_2O_3	44.2	16.2–57.5	45.5	18.3–56.7	43.8	15.5–61.9	44.6	26.6–57.6	63.5	26.2–71.4	64.0	55.2–72.3
NiO	2.1	0.6–9.6	2.1	0.7–8.6	2.2	0.6–9.5	3.4	0.6–8.6	2.4	0.6–9.1	2.6	0.2–11.0
ZnO	0.3	0.1–4.7							0.2	0.1–3.7		
Sum	100.0		100.0		100.0		100.0		100.0		100.0	
Fe^{3+}/Fe_{tot}	74.2	45.2–99.5	75.3	49.9–97.3	71.7	40.2–91.6	70.2	52.6–98.4	76.3	53.8–99.8	76.5	65.4–99.6

[a]Total number of randomly analyzed grains using SEM/EDS-ACC system.
All data in oxide wt% except Fe^{3+}/Fe_{tot} in element wt%.
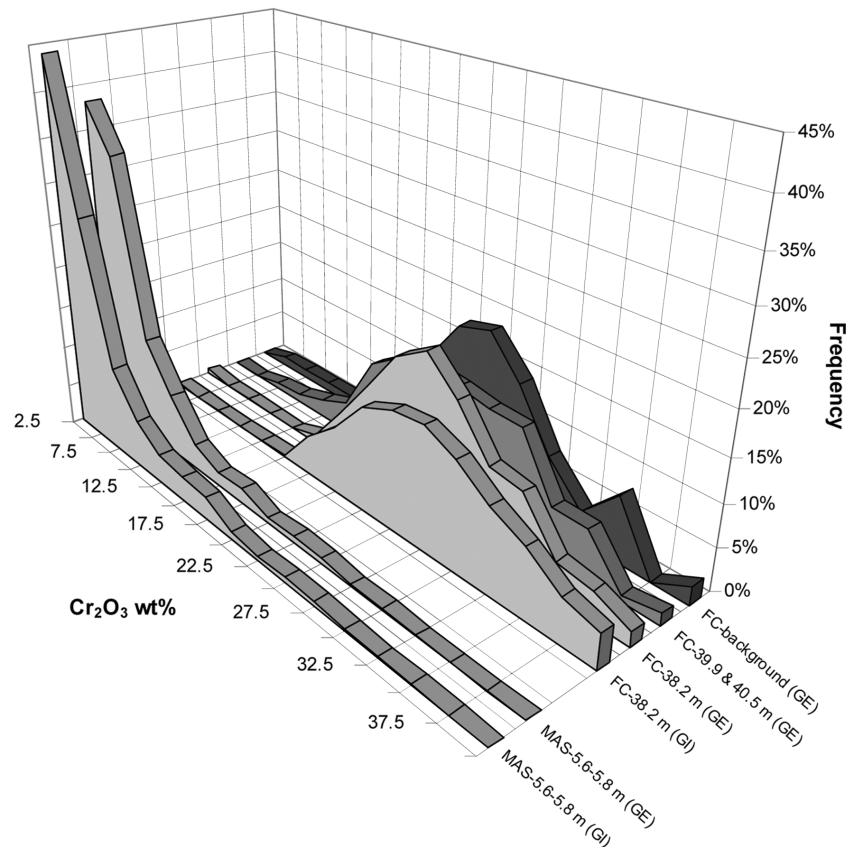FeO and Fe_2O_3 are calculated assuming a stoichiometric composition for spinel (Gayraud et al. 1996).

Fig. 6. Cr$_2$O$_3$ distributions of the Fuente Caldera (FC) and Massignano (MAS) spinel crystals (*AED* > 0.5 µm) recovered from the impact layers at 38.2 m and 5.6–5.8 m, respectively (GE and GI corresponding to grain exterior and interior analyses, respectively). Also shown are the Cr$_2$O$_3$ distributions of the Fuente Caldera spinel crystals (*AED* > 0.5 µm; grain exterior analyses) recovered from the 39.95 and 40.5 m layers, and the background.
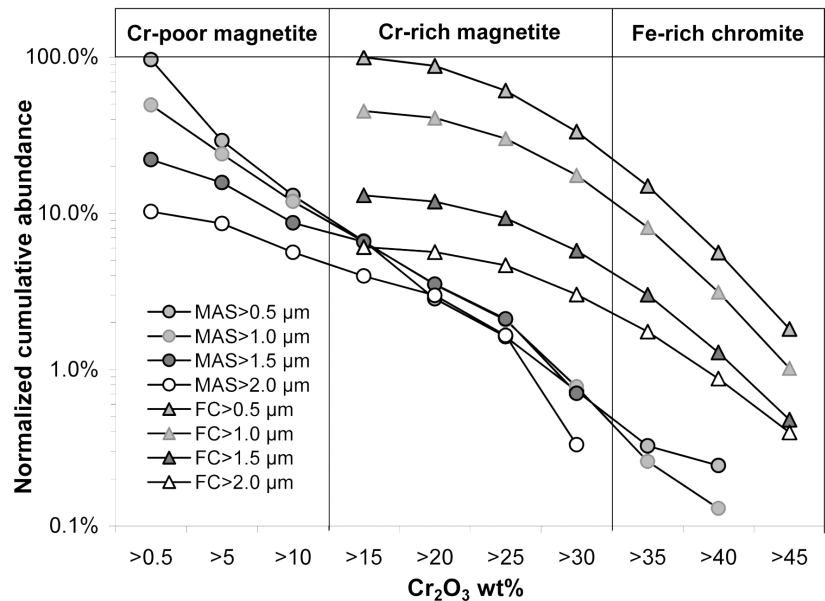

Fig. 7. Normalized cumulative Cr$_2$O$_3$ distributions of the Fuente Caldera (FC) and Massignano (MAS) spinel plotted for different crystal sizes (grain interior analyses).
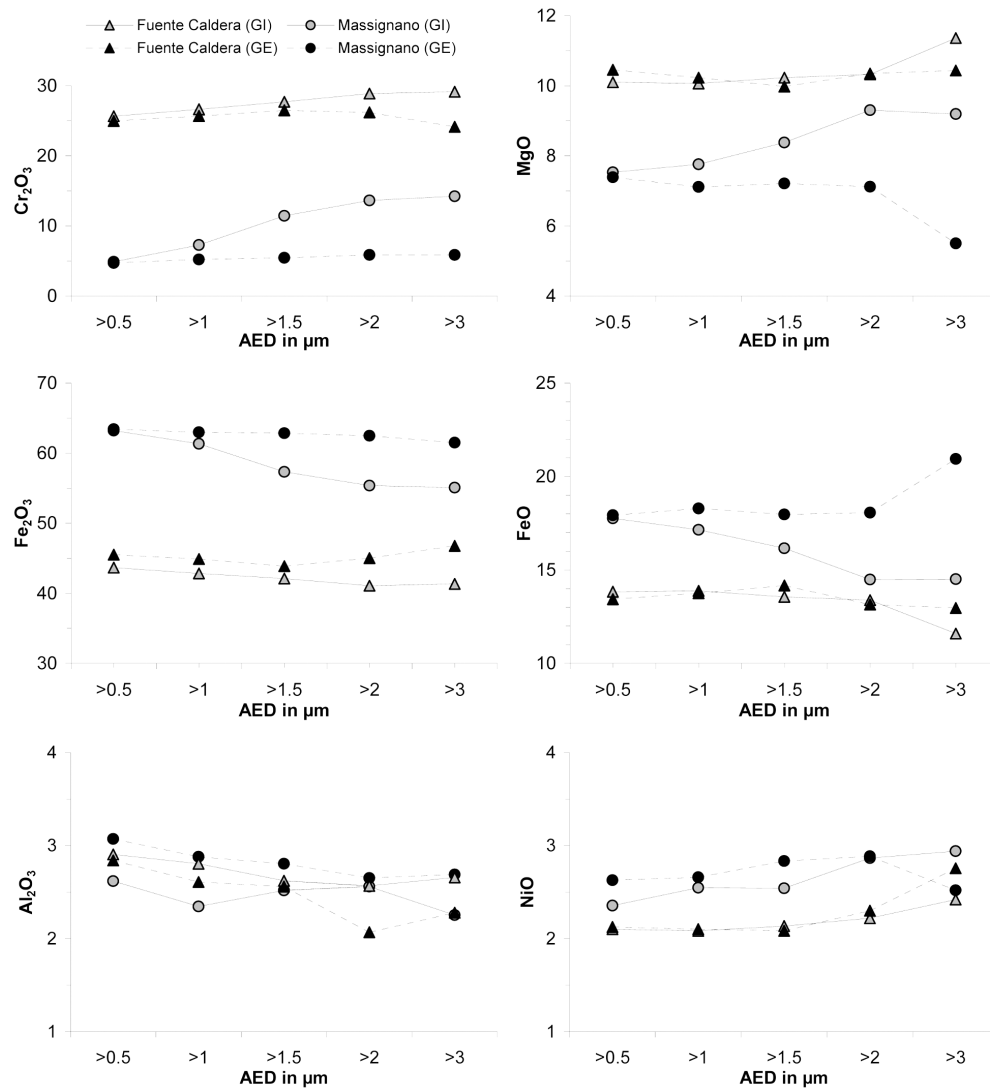
Fig. 8. A comparison between the internal (GI) and external (GE) average compositions of the Fuente Caldera and Massignano spinel calculated for different crystal sizes. Note that at both sites, grain exterior analyses show no compositional variation with the particle size. At Fuente Caldera, grain interior and exterior analyses are very similar reflecting the chemical homogeneity of the crystals. At Massignano, grain interior and exterior analyses reveal some Cr and Mg enrichments, and conversely Fe^{3+} and Fe^{2+} depletions, in the core of the particles >1.5 μm. Note that at both sites, no difference between the interior and the exterior of the grains, as well as no or only minor variations with the particle size, are observed for Al and Ni but also for Ti, Mn, and Fe^{3+}/Fe_{total} ratio (not shown).

series and less than 0.5% to the Fe-rich chromite series. As noticed by Pierrard et al. (1998), the spinel crystals at Massignano that belong to the Cr-rich magnetite series and the few ones that belong to the Fe-rich chromite series systematically show octahedral or skeletal morphologies. At this site, the crystals showing dendritic morphologies all belong to the Cr-poor magnetite series. At Fuente Caldera, the dendritic crystals and the octahedral and skeletal crystals all belong to the Cr-rich magnetite or Fe-rich chromite series. Apart from their different Cr concentrations, the Fuente Caldera and Massignano spinel crystals have quite comparable Al, Ti, Mn, and Ni concentrations and similar Fe^{3+}/Fe_{total} ratios.

It is important to note that the difference in the Cr

compositions of the Fuente Caldera and Massignano spinel cannot be attributed to a major sampling or analytical artifact, i.e., sampling of different size fractions or analysis of different parts of the grains, since they are observed on i) spinel grains that are in the same size range (Fig. 4), and ii) the innermost and outermost parts of the grains (Fig. 6; Table 2). However, the interior of some of the Massignano spinel crystals larger than 1.5 μm is clearly enriched in Cr and Mg, and conversely depleted in Fe^{3+} and Fe^{2+} compared to the exterior (Fig. 8). Such compositional differences cannot be attributed to some analytical artifacts because these arise from compositional variations of the interior of the largest grains, which were analyzed on polished sections and consequently are not subjected to analytical artifacts. At the opposite, grain
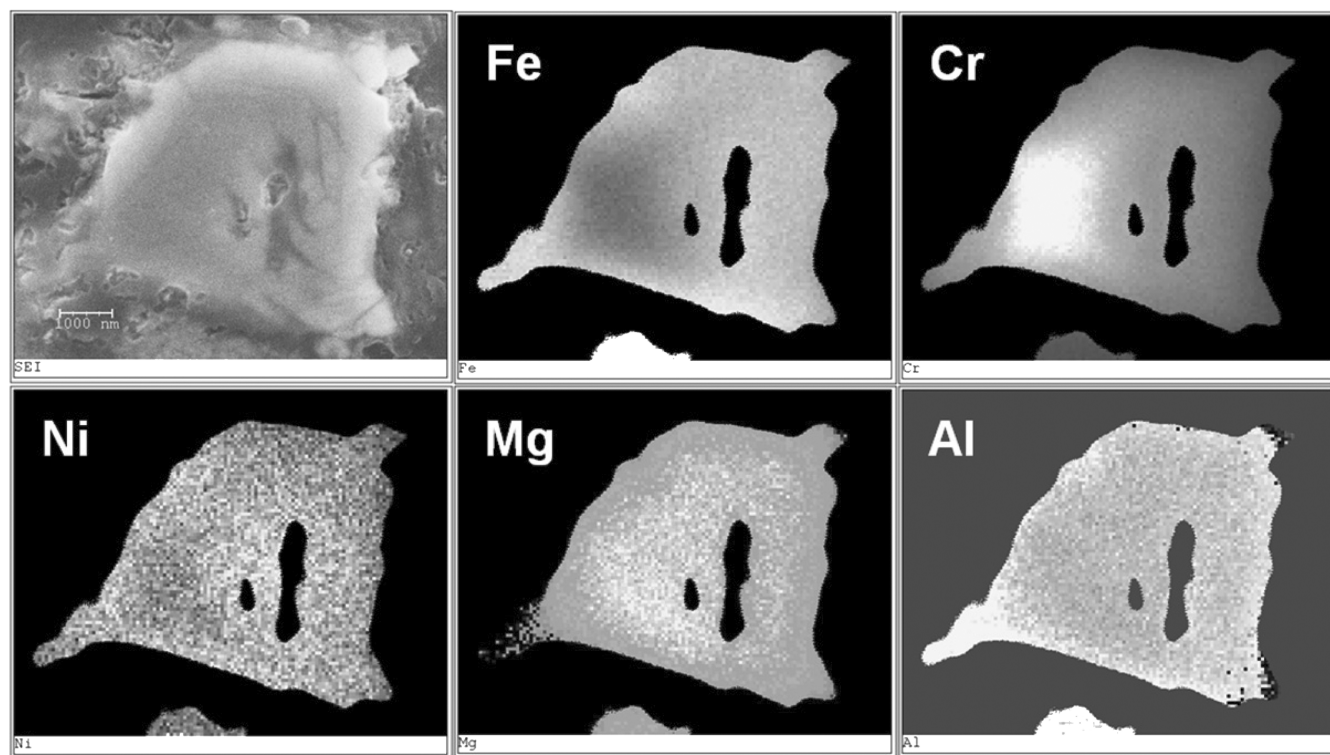
Fig. 9. Secondary electron image and X-ray maps for Fe, Cr, Ni, Mg, and Al of a large zoned spinel crystal (AED = 5 µm) recovered from the impact layer at Massignano.

exterior analyses, which are expected to be subjected to analytical artifacts (at least for particles >1 µm; see the Analytical Method section), show no variation with the particle size. At Fuente Caldera, the compositions of the interior and exterior of the grains are about similar with no major variations with the particle size. A small compositional difference between the interior and the exterior of the grains is however observed for some of the particles larger than 2–3 µm, the interior of which seems to be slightly enriched in Cr compared to the exterior. Note that at both sites no difference between the interior and the exterior of the grains, as well as no or only minor variations with the particle size, are observed for Al, Ti, Mn, Ni, and Fe^{3+}/Fe_{total} ratio.

SEM observations of the interior of the spinel crystals reveal the presence of Cr-rich core (Fig. 9) that likely account for the compositional differences observed between interior and the exterior of the grains. Indeed, these zonations are characterized by a decrease in Mg and Cr toward the margin with no or only minor variations in Al, Ni, and Fe^{3+}/Fe_{total} ratio. At both sites, the zoned crystals have lower Fe^{3+}/Fe_{total} ratios than the unzoned crystals with slightly higher Mg, lower Ni, and similar Al contents (Fig. 10). At Massignano, the Cr zonations seems to be restricted to the few octahedral and skeletal crystals that belong to the Cr-rich magnetite and Fe-rich chromite series (AED > 1.5 µm and Cr_2O_3 > 15 wt%; about 8% of the grains) (Fig. 7), the dendrites being chemically homogeneous. At Fuente Caldera,

the Cr zonations seems to be restricted to the few large spinel crystals (AED > 2 µm) belonging to the Fe-rich chromite series (Cr_2O_3 > 35 wt%; <2% of the grains), the other grains being chemically homogeneous.

DISCUSSION

Number and Age of Impact Horizons

In the Fuente Caldera section, three Ni-rich spinel horizons occur. If real, this would imply three distinct impact events within a short time interval of less than 60 kyr. However, several lines of evidence suggest that these three horizons all belong to the same impact event: 1) the chemical composition of the Ni-rich spinel in the three layers is very similar, 2) the spinel composition in the background is similar to the spinel composition in the three layers, and 3) the two upper layers are observed at the top of a sandstone layer of turbiditic origin. These considerations point to some erosion, local transport, and redeposition by turbiditic currents of a unique and single impact horizon.

Biostratigraphic correlations with the GSSP of Massignano give an age of 35.4 ± 0.2 Myr for the first spinel horizon (38.2 m) which likely corresponds to the age of the impact event that caused, through post-depositional processes, the spinel background distribution with two secondary spinel peaks in the Fuente Caldera section. This
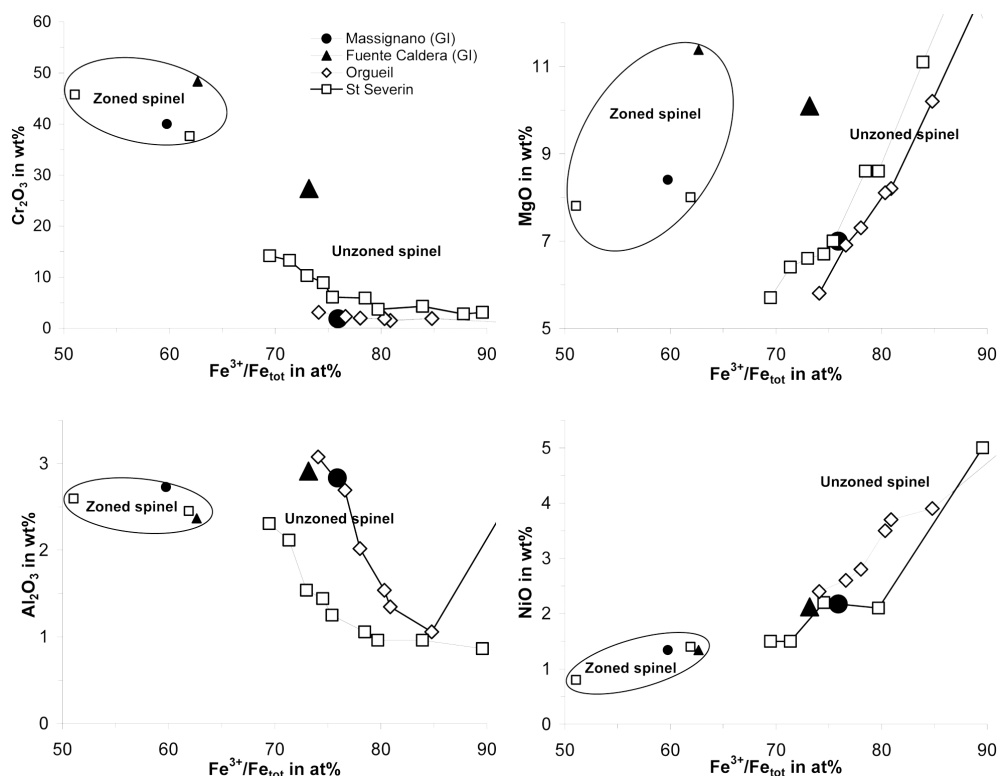
Fig. 10. Average spinel composition versus Fe^{3+}/Fe_{tot} ratios for zoned (small dots) and unzoned (large dots) crystals recovered from the impact layers at Fuente Caldera and Massignano. Also shown is the primary spinel composition for zoned and unzoned crystals synthetized from the Saint-Séverin and Orgueil meteorites (Gayraud 1995). The average composition of zoned spinel is calculated from Cr-rich core compositions measured in the largest crystals (*AED* > 2 μm; <10% of the grains). Note that the composition of zoned spinel at Massignano and, to a lesser extent at Fuente Caldera, is comparable to that of primary zoned spinel. Also, note that Al and Ni compositions of unzoned spinel at Fuente Caldera and Massignano are similar to those of primary unzoned spinel.

age is indistinguishable from the age of the impact event responsible of the spinel peak at Massignano (35.5 ± 0.2 Myr, Fig. 2) and is within uncertainties to the isotopic age of the Popigai crater (35.7 ± 0.2 Myr) and the biostratigraphic age of the Chesapeake Bay crater (35.5 ± 0.5 Myr).

Potential Source Craters

Previous studies have shown that Ni-rich spinel is present as a minor crystalline phase in microkrystites but has never been found inside microtektites, which are pure glass free of crystalline inclusions (Glass et al. 1985, 2004a; Glass and Burns 1988; Pierrard et al. 1999; Pierrard 1999; Vonhof and Smit 1999). Microkrystites and microtektites have not been found at Fuente Caldera and Massignano, but the Ni-rich spinel at Massignano is observed in flattened (pancake) spheroids (Pierrard et al. 1998) which are believed to be diagenetically altered microkrystites (Glass et al. 2004a). Extensive dissolution of microkrystites, leaving intact spinel only, may thus account for the occurrence of numerous "free" spinel crystals and the absence of microkrystites (and microtektites as well) in Fuente Caldera sediments. In the following, we assume that the Fuente Caldera spinel crystals

are the remnant after dissolution of microkrystites during diagenetic alteration.

At many sites, microkrystites and microtektites are mixed together in various proportions, except in Caribbean deep sea core RC9-58 (John and Glass 1974), DSDP site 612 (Glass 1989; Glass et al. 1998), ODP sites 903 and 904 (Glass et al. 1998), and at Gay's Cove North on Barbados (Pierrard 1999), where microkrystites and microtektites are found in two distinct layers, with the microkrystite layer lying about 25 cm below the microtektite layer. As discussed by Glass and co-workers (Glass et al. 1985), this stratigraphic separation is not the result of post-depositional processes as observed in Fuente Caldera because at Barbados the microkrystite horizon appears to be synchronous with the extinction of several radiolarian species, suggesting a short time interval (10–20 kyr) between the deposition of the microkrystite and microtektite layers. Microtektites from these sites are related to the North American tektite strewn field (Glass et al. 1985; Ngo et al. 1985), the origin of which is ascribed to the Chesapeake Bay crater (Koeberl et al. 1996). These considerations allow excluding the Chesapeake Bay crater as the source for microkrystites and therefore as a potential source for spinel.

It has been speculated that the Popigai impact crater may be the source for microkrystites (Glass 1997) and recent Sr and Nd isotopic data have been presented in support of a single microkrystite layer, global in extent, with a provenance from the Popigai impact crater (Whitehead et al. 2000; Liu et al. 2001; Kettrup et al. 2003). Our study provides additional evidence: at Fuente Caldera only one impact-related horizon is present, the age of which is indistinguishable from the age of the spinel horizon found at Massignano (35.5 ± 0.2 Myr) and within the age uncertainties for the Popigai (35.7 ± 0.2 Myr). We did not search for shock-metamorphosed mineral grains at Fuente Caldera, but at Massignano, shocked quartz (Clymer et al. 1996), the origin of which is attributed to the Popigai crater (Langenhorst and Clymer 1996; Glass et al. 2004a), and spinel-bearing microkrystites are present in the same layer (Glass et al. 2004a). Finally, the Popigai is large enough to have produced worldwide ejecta of impact spherules. Based on these considerations, the Popigai thus appears as a potential source for spinel.

On the other hand, if the Popigai is the source for the late Eocene spinel, why are spinel crystals from Fuente Caldera and Massignano so different in their composition and morphology? In particular, the absence of Cr-poor dendritic spinel crystals at Fuente Caldera, these latter being quite abundant at Massignano, is amazing if one considers that spinel crystals all derive from one large-body impact such as that at Popigai. Indeed, the idea that Popigai might spread millions of Cr-poor spinel crystals as far as Italy and not even one in Spain is apparently nonsensical. At least two explanations that are consistent with a unique source for spinel, can be proposed, namely, different modes of preservation or different modes of formation for this mineral.

Different Mode of Preservation?

One possible explanation of the difference in spinel compositions between Fuente Caldera and Massignano is that post-depositional alteration processes modified their original composition. We do not favor such an explanation because the morphologies of the Massignano and Fuente Caldera spinel crystals are in general comparable to those reported for primary spinel crystals, i.e., spinel crystals present in meteorite fusion crust or synthetized from meteoritic material. In particular, the dendritic morphology, which is the dominant morphology at Massignano, is a typical morphology of primary crystals that have crystallized in nonequilibrium conditions from a high temperature melt (Gayraud 1995; Gayraud et al. 1996). Moreover, the homogeneous Al and Ni compositions of the Massignano and Fuente Caldera spinel, with concentrations that are very similar to those in primary spinel (Fig. 10), even for the Fuente Caldera spinel that display Cr contents that are much higher than what is expected for primary spinel, are another evidence of the absence of spinel alteration. It is, however,

difficult to assess whether or not Ni-rich spinel crystals are altered and, if they are, to what extent alteration may have affected their Cr composition because of our poor knowledge of the alteration patterns in a mineral that is unique in the spinel group and for which few studies have been conducted. We can only rely on studies that describe alteration patterns in Cr-rich spinel from the terrestrial environment but these have been conducted on crystals that are i) less oxidized (Fe^{3+}/Fe_{tot} < 65 at%) and ii) much larger (>50 µm) than those studied here.

Alteration patterns in Cr-rich spinel from mafic and ultramafic rocks have been extensively described allowing the determination of three criteria that characterize spinel alteration (Burkhard 1993): 1) chemical inhomogeneities on a submicroscopic scale resulting from local dissolution; 2) zonation with a decrease in Mg, Al, and Cr towards the margin, and conversely an increase in Fe^{2+} and Fe^{3+}, which cannot be related to primary formation processes; and 3) significant concentrations of SiO_2 either correlated or inversely correlated with Cr_2O_3 contents. The first and third criteria are difficult to apply to Ni-rich spinel recovered from marly sediments because i) the small size of the crystals makes difficult the chemical characterization of possible submicroscopic inhomogeneities; and ii) detectable SiO_2 are positively correlated with K_2O reflecting significant contamination by the clay-rich surrounding matrix. SEM observations of the largest crystals show the occurrence of cracks and carve holes that could be indicative of local dissolution but the composition around them does not seem to be affected (Fig. 9). In addition, they have in general minor SiO_2 (0.1–0.6 wt%) that display no clear correlation with Cr_2O_3. However, most of the large spinel crystals are zoned with a decrease in Mg, Cr, and an increase in Fe^{2+} and Fe^{3+} from core to margin that could be related to alteration based on the second criterion. They also have a lower Ni and Fe^{3+}/Fe_{tot} ratios than the unzoned crystals but with no decrease, even a slight increase toward the margin. Similar chemical zonations are observed in spinel grains synthetized from the Saint-Séverin meteorite (Fig. 10) and are attributed to incomplete equilibration of relic chromite grains at subliquidus temperatures (Gayraud 1995). Note that these zoned grains also represent a small fraction (less than a few percent) of the total grains. It thus remains unclear whether the spinel zonations at Fuente Caldera and Massignano are related to primary crystallization or secondary alteration processes. We believe that these zonations are related to primary crystallization processes because their Al and Ni concentrations are very similar to those of primary zoned spinel (Fig. 10). Nevertheless, if they reflect secondary alteration processes, these have affected a few percents only of the total spinel grains (about 8% and less than 2% of the grains at Massignano and Fuente Caldera, respectively). It is therefore unlikely that the difference in the Cr composition between the Fuente Caldera and Massignano spinel arises from post depositional alteration processes.

Different Mode of Formation?

Several experimental (Hill and Roeder 1974; Murck and Campbell 1986; Gayraud et al. 1996; Toppani and Libourel 2003) and theoretical (Siret and Robin 2003; Siret 2004; Ebel and Grossman 2005) studies conducted on spinel crystallization have shown that the spinel composition is primarily controlled by the oxygen fugacity, temperature, and initial composition of the crystallizing material. Variable compositions in primary spinel crystals thus imply variations in the physical and chemical environment from which they were crystallized. Different types of environments can be considered depending on the mode of formation of impact spinel. For spinel-bearing spheroids found at the Cretaceous/Paleogene boundary, two potential modes of formation have been proposed namely including condensation in the impact vapor plume (Kyte and Smit 1986) and atmospheric ablation of mixed projectile/target debris (Robin et al. 1992).

Assuming vapor condensation as the main mode of formation, spatial variations may account for if material from different localities was derived from different regions in the vapor cloud, the temperature, oxygen fugacity and compositions of which evolve during vapor expansion. This scenario has been proposed to explain the regional trends in spinel compositions observed over the entire Pacific basin at the Cretaceous/Paleogene boundary (Kyte et al. 1996) and is supported by recent theoretical considerations showing that the Chicxulub vapor cloud might have produced the kind of environment required for spinel crystallization (Ebel and Grossman 2005).

On the other hand, Robin and co-workers pointed out that this scenario is difficult to reconcile with i) the finding of partially melted meteoritic debris rimmed with spinel crystals which obviously cannot result from vapor condensation (Robin et al. 1993), and ii) the local variations in spinel compositions as observed at several Cretaceous/Paleogene Tethyan sites separated by less than a few tens of kilometers (Robin and Rocchia 1998; Robin et al. 1999). These authors suggest instead that spinel is locally derived and crystallized in material generated by the ablation of mixed projectile/target debris ejected from the impact site and reentering the Earth's atmosphere. This scenario is consistent with laboratory experiments (Schultz and Gault 1982, 1990) and hydrocode modeling (Pierazzo and Melosh 2000) of oblique impacts showing that a large fraction (>70%) of the projectile survives the impact in the solid and liquid state and is rapidly expelled from the crater by the expanding vapor from the shocked target. High-velocity interaction with the atmosphere for meteoritic material is known as a source for Ni-rich spinel (Robin et al. 1992; Gayraud et al. 1996). It is therefore likely that atmospheric reentry of mixed projectile/target impact debris is a source for this mineral. In this scenario, the temperature and oxygen fugacity experienced by the reentering debris as well as the composition of the crystallizing material depend on the size, velocity, density, entry angle, and projectile/target ratio, which may vary from place to place, accounting for spatial variations in spinel compositions.

Although we do not exclude vapor condensation as a potential source for the late Eocene spinel, we are forced to say that, here again, this scenario is difficult to reconcile with the spatial variations in spinel compositions as observed between Massignano and Fuente Caldera. Even if one considers a highly heterogeneous vapor cloud, we should expect large compositional overlap at least between Fuente Caldera and Massignano. Indeed, condensed material ejected from the Popigai crater and deposited at both sites (about 6500 ± 500 km away) arrives along very similar trajectories (both sites are virtually aligned with the Popigai and distant one from the other by less than 1000 km) and, because of the wide angular dispersion of the particle velocities (Pierazzo and Melosh 2000), we should expect the contribution at both sites of material from different regions of the cloud. This is not what we observed: the Cr-poor spinel at Massignano, which represents more than 90% of the total spinel grains ($Cr_2O_3 < 15$ wt%) (Fig. 7), is not recorded in the investigated section at Fuente Caldera. This implies that a large fraction of the Massignano spinel would originate from a portion of the vapor cloud that is quite distinct from the one that produced the Fuente Caldera spinel. If so, it is required to imagine a very selective process bringing microkrystites (50–500 μm in size) from a given portion of the Popigai vapor cloud to a restricted region in Europe. We believe that local reentry of impact debris of heterogeneous composition better account for the wide geographical variability in the chemical composition of spinel as well as in the chemical and isotopic compositions of microtektites and microkrystites.

Different Impact Events?

An alternative explanation is that Fuente Caldera and Massignano spinel crystals originate from two distinct impacts. This explanation cannot be discarded because the chemical and isotopic data presented in the literature do not clearly demonstrate whether the different microkrystite horizons found at many sites worldwide all derive from the Popigai crater. Indeed, microkrystites from the different sites investigated so far—three from the Pacific Ocean, three from the Indian Ocean, and one from the Atlantic Ocean (Whitehead et al. 2000; Liu et al. 2001)—display a wide range of isotopic compositions compared to the narrow range of values measured for the Popigai melt rocks, i.e., the so-called Popigai tagamites (Kettrup et al. 2003). For instance, microkrystites from DSDP site 292 and DSDP site 315, in the western and central equatorial Pacific Ocean, respectively, display two distinct isotopic signatures, both being distinct from the field defined by the range of values of the Popigai

tagamites. In fact, except for DSDP site 462 in the equatorial Pacific Ocean, none of the six remaining sites fall within the field of the Popigai tagamites (Liu et al. 2001). Moreover, the chemical composition of the microkrystites does not match with mixtures of basement rocks and overlying sediments (for which compositional data are available) at the Popigai impact crater (Glass et al. 2004b). The question of the number and source of microtektite horizons also merits re-examination in light of the chemical and isotopic data. Indeed, microtektites from ODP site 689 and DSDP site 216, in the southern and eastern Indian Ocean, respectively, display two distinct isotopic signatures, both being distinct from the field defined by the range of values of the North American tektites and microtektites. Instead, the isotopic signature of the microtektites from these two sites falls within the field defined by microkrystites, though for a given site both components have a distinct isotopic signature (Whitehead et al. 2000; Liu et al. 2001).

It has been argued that the wide variability in the microkrystite chemical and isotopic compositions may simply reflect melting with incomplete homogenization of the chemically and isotopically diverse Popigai target rocks (Whitehead et al. 2000; Kettrup et al. 2003). Another argument often raised to account for the compositional differences between Popigai melt rocks and microkrystites is that the former are derived from the basement rocks whereas the latter are derived from the sedimentary cover rocks for which few data are available. Note that these arguments may also apply to account for the compositional diversity of microtektites assuming derivation from the Chesapeake Bay crater (Glass et al. 2004b). However, these arguments may also apply assuming derivation from the Late Eocene Mistastin crater (Canada, 36.4 ± 4 Myr, 28 km), this one being presently discarded because the melt rock composition is distinct from that of the microkrystites and microtektites (Whitehead et al. 2000).

It appears that the spatial variability in the chemical and isotopic signatures of the microkrystites and in the chemical composition of spinel does not clearly resolve whether these impact markers form a unique horizon, global in extent, with a provenance from the Popigai (though it does not exclude this possibility) or distinct horizons, local or global in extent, with a provenance from temporally or geographically distinct impact events. At Massignano, evidence of temporally spaced impact events is given by the occurrence of three distinct impact horizons. Indeed, in addition to the Cr-poor spinel horizon at 5.7 m, two other impact horizons have been reported at 6.2 and 10.3 m (Montanari et al. 1993; Bodiselitsch et al. 2004). The second horizon at 6.2 m is ≈70 kyr younger than the Cr-poor spinel horizon at 5.7 m and is tentatively related to the Chesapeake Bay impact event (Bodiselitsch et al. 2004). However, this cratering event is considered as the source of the North American microtektites that are not associated with an Ir anomaly (Glass et al. 1985).

If so, the younger impact horizon at Massignano is derived from another, so far unknown, impact crater. There are some potential candidates but these are presently discarded because of the large uncertainties attached to their age (for instance Logancha and Beyenchime-Salaatin, Russia, 40 ± 20 Myr) or because these are, in theory, not large enough to spread ejecta material over large areas (for instance Chiyli, Kazakhstan, 5.5 km). It is not clear whether the second Ir anomaly at Massignano is associated with spinel. Pierrard et al. (1998) reported a relatively high spinel background for this section (≈1–2 crystal/mg compared to <0.05 crystal/mg at Fuente Caldera), corresponding to a maximum spinel flux of $\approx 10^5$ crystals/cm^2 in the 6.1–6.3 m stratigraphic interval. However, as far as we know, no detailed stratigraphic distribution and no chemical analysis of the spinel crystals have been reported for this interval. At Fuente Caldera, we observed one spinel horizon only, but whether distinct spinel horizons are all recorded and preserved is questionable because of recurrent and closely spaced (every 10–60 kyr) (Table 2; Fig. 3) turbiditic events that may have eroded some of them. Consequently, whether the Cr-rich spinel horizon at Fuente Caldera is correlated to the Cr-poor spinel horizon or to a potentially younger spinel horizon at Massignano remains questionable.

CONCLUSIONS

Our study of the stratigraphic distribution and chemical composition of Ni-rich spinel in the Fuente Caldera section in Spain led to the following conclusions:

1. The series of Ni-rich spinel horizons recorded at Fuente Caldera in the biostratigraphic interval defined by the last occurrence of the planktic foraminifera *P. semiinvoluta* and the first occurrence of the planktic foraminifera *T. cunialensis* likely results from the erosion, local transport, and redeposition by turbiditic currents of a unique and single impact horizon.

2. This horizon is dated at 35.4 ± 0.2 Myr and is about coeval with the spinel horizon recorded in the global stratotype section and point for the Eocene/Oligocene boundary of Massignano in Italy, the origin of which is ascribed to the Popigai impact crater.

3. The morphologies and Cr compositions of the Fuente Caldera and Massignano spinel crystals are, however, markedly different. It is unlikely that these differences result from different post-depositional alteration processes because the morphologies and compositions of the Fuente Caldera and Massignano spinel crystals are in general very similar to those of primary spinel crystals, i.e., spinel crystals present in meteorite fusion crust or synthetized from meteoritic material. In addition, spinel crystals have quite homogeneous compositions except for a few grains (<10%) showing Cr zonations but these are assigned to primary crystallization processes.

4. Spatial variations in spinel morphologies and Cr compositions likely reflect different modes of formation for this mineral. Considering a single impact, this may be accounted for assuming that microkrystites, the alleged carrier of spinel crystals, were locally generated by the ablation in the atmosphere of impact debris. An alternative explanation is that Fuente Caldera and Massignano microkrystites derive from two closely spaced impact-generated microkrystite events. If so, another so-far unknown impact-generated microkrystite event is required.

Editorial Handling—Dr. Alexander Deutsch

REFERENCES

Asaro F., Alvarez L. W., Alvarez W., and Michel H. V. 1982. Geochemical anomalies near the Eocene/Oligocene and Permian/Triassic boundaries. GSA Special Paper #190. Boulder, Colorado: Geological Society of America. pp. 517–528.

Bodiselitsch B., Montanari A., Koeberl C., and Coccioni R. 2004. Delayed climate cooling in the Late Eocene caused by multiple impacts: High-resolution geochemical studies at Massignano, Italy. *Earth and Planetary Science Letters* 223:283–302.

Burkhard D. J. M. 1993. Accessory chromium spinels: Their coexistence and alteration in serpentinites. *Geochimica et Cosmochimica Acta* 57:1297–1306.

Clymer A. K., Bice D. M., and Montanari A. 1996. Shocked quartz from the late Eocene: Impact evidence from Massignano, Italy. *Geology* 24:483–486.

Collins G. S. and Wünnemann K. 2005. How big was the Chesapeake Bay impact? Insight from numerical modeling. *Geology* 33:925–928.

Deutsch A. and Koeberl C. 2006. Establishing the link between the Chesapeake Bay impact structure and the North American tektite strewn field: The Sr-Nd isotopic evidence. *Meteoritics & Planetary Science* 41:689–703.

Ebel D. S. and Grossman L. 2005. Spinel-bearing spherules condensed from the Chicxulub impact-vapor plume. *Geology* 33:293–296.

Farley K. A., Montanari A., Shoemaker E. M., and Shoemaker C. S. 1998. Geochemical evidence for a comet shower in the late Eocene. *Science* 280:1250–1253.

Ganapathy R. 1982. Evidence for a major meteorite impact on the Earth 34 million years ago: Implication on the origin of North American tektites and Eocene extinction. GSA Special Paper #190. Boulder, Colorado: Geological Society of America. pp. 513–516.

Gayraud J., Robin E., Rocchia R., and Froget L. 1996. Formation conditions of oxidized Ni-rich spinel and their relevance to the K/T boundary event. GSA Special Paper #307. Boulder, Colorado: Geological Society of America. pp. 425–443.

Glass B. P. 1989. North American tektite debris and impact ejecta from DSDP Site 612. *Meteoritics* 24:209–218.

Glass B. P. 1990. Chronostratigraphy of upper Eocene microspherules. Comment and Reply. *Palaios* 5:387–390.

Glass B. P. 1997. Source rock and meteoritic contamination of upper Eocene clinopyroxene-bearing spherules (abstract). *Meteoritics & Planetary Science* 32:A49.

Glass B. P. and Burns C. A. 1987. Late Eocene crystal-bearing spherules: Two layers or one? *Meteoritics* 22:265–279.

Glass B. P. and Burns C. A. 1988. Microkrystites: A new term for impact-produced glassy spherules containing primary crystallites. Proceedings, 18th Lunar and Planetary Science Conference. pp. 455–458.

Glass B. P. and Koeberl C. 1999. Ocean Drilling Project Hole 689B spherules and upper Eocene microtektite and clinopyroxene-bearing spherule strewn fields. *Meteoritics & Planetary Science* 34:197–208.

Glass B. P. and Wu J. 1993. Coesite and shocked quartz discovered in the Australasian and North American microtektite layers. *Geology* 21:435–438.

Glass B. P., Baker R. N., Storzer D., and Wagner G. A. 1973. North American microtektites from the Caribbean Sea and Gulf of Mexico. *Earth and Planetary Science Letters* 19:184–192.

Glass B. P., Dubois D. L., and Ganapathy R. 1982. Relationship between an iridium anomaly and the North American microtektites layer in core RC9-58 from the Caribbean Sea. Proceedings, 13th Lunar and Planetary Science Conference. pp. A425–A428.

Glass B. P., Burns C. A., Crosbie J. R., and Dubois D. L. 1985. Late Eocene North American microtektites and clinopyroxene-bearing spherules. Proceedings, 15th Lunar and Planetary Science Conference. pp. D175–D196.

Glass B. P., Koeberl C., Blum J. D., and McHugh M. G. 1998. Upper Eocene tektite and impact ejecta layer on the continental slope off New Jersey. *Meteoritics & Planetary Science* 33:229–241.

Glass B. P., Liu S., and Montanari A. 2004a. Impact ejecta in upper Eocene deposits at Massignano, Italy. *Meteoritics & Planetary Science* 39:589–597.

Glass B. P., Huber H., and Koeberl C. 2004b. Geochemistry of Cenozoic microtektites and clinopyroxene-bearing spherules. *Geochimica et Cosmochimica Acta* 68:3971–4006.

Hazel J. E. 1989. Chronostratigraphy of upper Eocene microspherules. *Palaios* 4:318–329.

Hill R. and Roeder P. 1974. The crystallization of spinel from basaltic liquid as a function of oxygen fugacity. *Journal of Geology* 82:709–729.

Jéhanno C., Boclet D., Bonté P., Castellarin A., and Rocchia R. 1988. Identification of two populations of extraterrestrial particles in a Jurassic hardground of the southern Alps. Proceedings, 18th Lunar and Planetary Science Conference. pp. 623–630.

John C. and Glass B. P. 1974. Clinopyroxene-bearing glass spherules associated with North American microtektites. *Geology* 2:599–602.

Keller G., D'Hondt S. L., Orth C. J., Gilmore J. S., Oliver P. Q., Shoemaker E. M., and Molina E. 1987. Late Eocene impact microspherules: Stratigraphy, age and geochemistry. *Meteoritics* 22:25–60.

Kettrup B., Deutsch A., and Masaitis V. L. 2003. Homogeneous impact melts produced by a heterogeneous target? Sr-Nd isotopic evidence from the Popigai crater, Russia. *Geochimica et Cosmochimica Acta* 67:733–750.

Koeberl C., Poag C. W., Reimold W. U., and Brandt D. 1996. Impact origin of the Chesapeake Bay structure and the source of the North American tektites. *Science* 271:1263–1266.

Kyte F. T. and Bostwick J. A. 1995. Magnesioferrite spinel in Cretaceous/Tertiary boundary sediments of the Pacific basin: Remnants of hot, early ejecta from the Chicxulub impact. *Earth and Planetary Science Letters* 132:113–127.

Kyte F. T. and Smit J. 1986. Regional variations in spinel compositions: An important key to the Cretaceous/Tertiary event. *Geology* 14:485–487.

Kyte F. T., Bostwick J. A., and Zhou L. 1996. The Cretaceous-Tertiary boundary on the Pacific plate: Composition and distribution of impact debris. GSA Special Paper #307. Boulder, Colorado: Geological Society of America. pp. 389–415.

Langenhorst F. and Clymer A. 1996. Characteristics of shocked quartz in late Eocene impact ejecta from Massignano (Ancona, Italy): Clues to shock conditions and source crater. *Geology* 24: 487–490.

Liu S., Glass B. P., Ngo H. H., Papanastassiou D. A., and Wasserburg G. J. 2001. Sr and Nd data for upper Eocene spherule layers (abstract #1819). 32nd Lunar and Planetary Science Conference. CD-ROM.

Margolis S. V., Claeys P., and Kyte F. T. 1991. Microtektites, microkrystites, and spinels from a Late Pliocene asteroid impact in the Southern Ocean. *Science* 251:1594–1597.

Masaitis V. L., Naumov M. V., and Mashchak M. S. 1999. Anatomy of the Popigai crater, Russia. GSA Special Paper #339. Boulder, Colorado: Geological Society of America. pp. 1–17.

Molina E. 1986. Description and biostratigraphy of the main reference section of the Eocene/Oligocene boundary in Spain: Fuente Caldera section. In *Terminal Eocene events,* edited by Pomerol C. and Premoli-Silva I. New York: Elsevier. pp. 53–63.

Molina E., Gonzalvo C., and Keller G. 1993. The Eocene-Oligocene planktic foraminiferal transition: Extinction, impacts and hiatuses. *Geological Magazine* 4:483–499.

Molina E., Cruz L. E., Gonzalvo C., Ortiz S., and Robin E. 2004. Evidencias de impacto meteoritico en el Eoceno Superior de Fuente Caldera (Granada, Cordilleras Béticas). *Geo-Temas* 6: 365–368.

Monechi S. 1986. Biostratigraphy of Fuente Caldera section by means of calcareous nanofossils. In *Terminal Eocene events,* edited by Pomerol C. and Premoli-Silva I. New York: Elsevier. pp. 53–63.

Montanari A., Asaro F., Michel H. V., and Kennett J. P. 1993. Iridium anomalies of Late Eocene age at Massignano (Italy), and ODP site 689B (Maud Rise, Antarctica). *Palaios* 8:420–437.

Murck B. and Campbell I. H. 1986. The effects of temperature, oxygen fugacity and melt composition on the behavior of chromium in basic and ultrabasic melts. *Geochimica et Cosmochimica Acta* 50:1871–1887.

Ngo H. H., Wasserburg G. J., and Glass B. P. 1985. Nd and Sr isotopic composition of tektite material from Barbados and their relationship to North American tektites. *Geochimica et Cosmochimica Acta* 49:1429–1485.

Pierazzo E. and Melosh H. J. 2000. Hydrocode modeling of oblique impacts: The fate of the projectile. *Meteoritics & Planetary Science* 35:117–130.

Pierrard O. 1999. Etude du phénomène cosmique de la fin de l'Eocene et recherche d'une corrélation avec les modifications du climat et de l'environnement. Ph.D. thesis, Université d'Orsay, Paris XI, France.

Pierrard O., Robin E., and Montanari A. 1998. Extraterrestrial Ni-rich spinel in upper Eocene sediments from Massignano, Italy. *Geology* 26:307–310.

Pierrard O., Robin E., Rocchia R., Lefevre I., Smit J., and Vonhof H. 1999. Late Eocene Ni-rich spinel from LL44-GPC3 (Central Pacific), ODP site 689B (Maud Rise, Antarctica), DSDP sites 94 (Gulf of Mexico) and 612 (U.S. East Coast) (abstract #964). 30th Lunar and Planetary Science Conference. CD-ROM.

Robin E. and Rocchia R. 1998. Ni-rich spinel at the Cretaceous-Tertiary boundary of El Kef, Tunisia. *Bulletin Société Géologique de France* 169:365–372.

Robin E., Boclet D., Bonté P., Froget L., Jéhanno C., and Rocchia R. 1991. The stratigraphic distribution of Ni-rich spinels in Cretaceous-Tertiary boundary rocks at El Kef (Tunisia), Caravaca (Spain) and hole 761C (Leg 122). *Earth and Planetary Science Letters* 107:715–721.

Robin E., Bonté P., Froget L., Jéhanno C., and Rocchia R. 1992. Formation of spinels in cosmic objects during atmospheric entry: A clue to the Cretaceous-Tertiary boundary event. *Earth and Planetary Science Letters* 108:181–190.

Robin E., Froget L., Jéhanno C., and Rocchia R. 1993. Evidence for a K/T impact event in the Pacific Ocean. *Nature* 363:615–617.

Robin E., Rocchia R., Lefèvre I., Pierrard O., Dupuis C., Smit J., Zaghbib-Turki D., and Matmati F. 1999. Local variations in spinel compositions at the K/T boundary in Tunisia: Evidence for long range dispersion of impact debris (abstract #964). 30th Lunar and Planetary Science Conference. CD-ROM.

Rocchia R., Robin E., Froget L., and Gayraud J. 1996. Stratigraphic distribution of extraterrestrial markers at the Cretaceous-Tertiary boundary in the Gulf of Mexico area: Implications for the temporal complexity of the event. GSA Special Paper #307. Boulder, Colorado: Geological Society of America. pp. 279–286.

Schultz P. H. and Gault D. E. 1982. Impact ejecta dynamics in an atmosphere: Experimental results and extrapolations. GSA Special Paper #190. Boulder, Colorado: Geological Society of America. pp. 153–174.

Schultz P. H. and Gault D. E. 1990. Prolonged global catastrophes from oblique impacts. GSA Special Paper #247. Boulder, Colorado: Geological Society of America. pp. 239–262.

Siret D. 2004. Evaluation des rejets atmosphériques engendrées par un impact météoritique: Approche thermodynamique. Ph.D. thesis, Université Denis Diderot, Paris VII, France.

Siret D. and Robin E. 2003. Spinel formation in an impact plume: A thermodynamic approach (abstract #1865). 34th Lunar and Planetary Science Conference. CD-ROM.

Smit J. and Kyte F. T. 1984. Siderophile-rich magnetic spheroids from the Cretaceous-Tertiary boundary in Umbria, Italy. *Nature* 310:403–405.

Toppani A. and Libourel G. 2003. Factors controlling compositions of cosmic spinels: Application to atmospheric entry conditions of meteoritic materials. *Geochimica et Cosmochimica Acta* 67: 4621–4638.

Vonhof H. B., and Smit J. 1999. Late Eocene microkrystites and microtektites at Maud Rise (O.D.P. hole 689B; Southern Ocean) suggest a global extension of the approximately 35.5 Ma Pacific impact ejecta strewn field. *Meteoritics & Planetary Science* 34: 747–755.

Wei W. 1995. How many impact-generated microspherule layers in the upper Eocene? *Palaeogeography, Palaeoclimatology, Palaeoecology* 114:101–110.

Whitehead J., Papanastassiou D. A., Spray J. G., Grieve R. A. F., and Wasserburg G. J. 2000. Late Eocene impact ejecta: Geochemical and isotopic connections with the Popigai impact structure. *Earth and Planetary Science Letters* 181:473–487.